Arabidopsis J-Protein J20 Delivers the First Enzyme of the Plastidial Isoprenoid Pathway to Protein Quality Control[C][W]

Pablo Pulido,[a] Gabriela Toledo-Ortiz,[a,1] Michael A. Phillips,[a] Louwrance P. Wright,[b] and Manuel Rodríguez-Concepción[a,2]

[a] Centre for Research in Agricultural Genomics, CSIC-IRTA-UAB-UB, 08193 Barcelona, Spain
[b] Max Planck Institute for Chemical Ecology, 07745 Jena, Germany

ORCID IDs: 0000-0001-9092-3674 (P.P.); 0000-0002-1280-2305 (M.R-C.).

Plastids provide plants with metabolic pathways that are unique among eukaryotes, including the methylerythritol 4-phosphate pathway for the production of isoprenoids essential for photosynthesis and plant growth. Here, we show that the first enzyme of the pathway, deoxyxylulose 5-phosphate synthase (DXS), interacts with the J-protein J20 in *Arabidopsis thaliana*. J-proteins typically act as adaptors that provide substrate specificity to heat shock protein 70 (Hsp70), a molecular chaperone. Immunoprecipitation experiments showed that J20 and DXS are found together in vivo and confirmed the presence of Hsp70 chaperones in DXS complexes. Mutants defective in J20 activity accumulated significantly increased levels of DXS protein (but no transcripts) and displayed reduced levels of DXS enzyme activity, indicating that loss of J20 function causes posttranscriptional accumulation of DXS in an inactive form. Furthermore, J20 promotes degradation of DXS following a heat shock. Together, our data indicate that J20 might identify unfolded or misfolded (damaged) forms of DXS and target them to the Hsp70 system for proper folding under normal conditions or degradation upon stress.

INTRODUCTION

A complex network of biosynthetic pathways in different subcellular compartments supports plant life. In particular, plastids provide a number of unique metabolic pathways among eukaryotes, including the methylerythritol 4-phosphate (MEP) pathway for the production of isoprenoid precursors. MEP-derived isoprenoids (Figure 1) include compounds essential for photosynthesis (such as carotenoids and the side chain of chlorophylls, tocopherols, plastoquinone, and phylloquinone) and growth regulation (including the hormones gibberellin, cytokinin, strigolactone, and abscisic acid). The importance of the MEP pathway extends beyond its essential role for plant life and includes precursors to health-promoting phytonutrients, drugs, and industrial raw materials. Thus, metabolic engineering of the MEP pathway in plants has increased the production of plastidial isoprenoids of nutritional and economic relevance (Botella-Pavía and Rodríguez-Concepción, 2006; DellaPenna and Pogson, 2006). The first reaction of the MEP pathway involves the synthesis of deoxyxylulose 5-phosphate (DXP) from the central metabolic intermediates glyceraldehyde 3-phosphate and pyruvate (Sprenger et al., 1997; Lange et al., 1998; Lois et al., 1998). This reaction is catalyzed by DXP synthase (DXS), an enzyme encoded by the *CLOROPLASTOS ALTERADOS1* (*CLA1*)/*CHILLING-SENSITIVE5* (*CHS5*)/*DXS* (At4g15560) gene in *Arabidopsis thaliana* (Mandel et al., 1996; Araki et al., 2000; Estévez et al., 2000). The intramolecular rearrangement and reduction of DXP by DXP reductoisomerase (DXR) yields MEP (Kuzuyama et al., 1998; Takahashi et al., 1998). DXR is also encoded by a single *Arabidopsis* gene, At5g62790 (Schwender et al., 1999; Carretero-Paulet et al., 2002). MEP is converted to the C5 isoprenoid precursors isopentenyl diphosphate and dimethylallyl diphosphate in five additional steps (reviewed in Rodríguez-Concepción and Boronat, 2002). It is likely that several enzymes share control over the flux of the MEP pathway, with different enzymes exhibiting different degrees of control, as suggested by metabolic control analysis models. Consistent with this, both DXS and DXR have been shown to increase the production of final isoprenoid products when overexpressed in transgenic plants (Lois et al., 2000; Estévez et al., 2001; Mahmoud and Croteau, 2001; Rodríguez-Concepción et al., 2001; Enfissi et al., 2005; Carretero-Paulet et al., 2006; Muñoz-Bertomeu et al., 2006). Therefore, the metabolic control analysis term rate-determining can be applied to both enzymes.

In addition to the coarse regulation exerted by changes in gene expression, fine modulation of MEP pathway enzyme abundance takes place at the posttranscriptional level (Laule et al., 2003; Guevara-García et al., 2005; Sauret-Güeto et al., 2006; Flores-Pérez et al., 2008, 2010; Cordoba et al., 2009; Rodríguez-Villalón et al., 2009; Pulido et al., 2012; Hemmerlin, 2013). However, we still know little about the specific mechanisms that determine the levels of active enzymes. All of the MEP pathway enzymes are encoded in the nuclear genome, and the corresponding preproteins are imported into plastids upon their synthesis. Once imported, their plastid targeting peptides are cleaved and the mature proteins are presumed to be folded to their active form. However, protein misfolding is an inevitable process aggravated by environmental stresses, such as heat shock. In response to this problem, protein quality control systems composed of molecular chaperones and
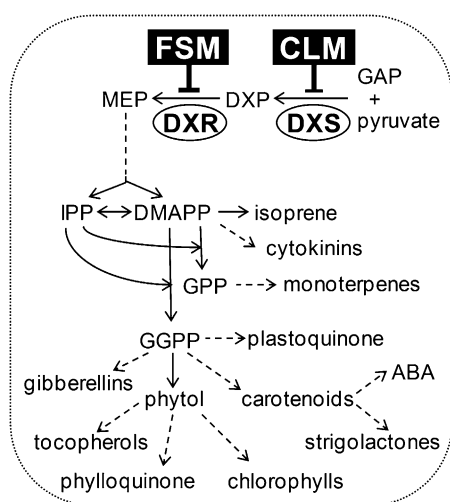
Figure 1. Isoprenoid Biosynthesis in Plastids.

The MEP pathway produces the universal isoprenoid precursors isopentenyl diphosphate (IPP) and dimethylallyl diphosphate (DMAPP). The production of DXP from pyruvate and glyceraldehyde 3-phosphate (GAP) by the enzyme DXS can be blocked with CLM, whereas the production of MEP from DXP catalyzed by DXR can be inhibited by fosmidomycin (FSM). Condensation of IPP and DMAPP units produces prenyl diphosphates of increasing size, such as geranyl diphosphate (GPP) and geranylgeranyl diphosphate (GGPP), which are the starting points for the biosynthesis of isoprenoid end-products. Dashed open arrows represent multiple biosynthetic steps.

proteolytic complexes have evolved to either refold or eliminate misfolded proteins and thereby maintain protein homeostasis. A number of chaperone and protease systems are found in chloroplasts (Boston et al., 1996; Kato and Sakamoto, 2010; Nordhues et al., 2010), but their relevance for plastidial metabolism in general and isoprenoid biosynthesis in particular awaits further investigation.

In this work we report that *Arabidopsis* J20, a J-protein (or DnaJ-like protein), acts as an adaptor that recognizes inactive forms of DXS and delivers them to the heat shock protein 70 (Hsp70) molecular chaperone. We propose that this mechanism likely drives proper folding of DXS for enzymatic activation while also facilitating the removal of defective forms of the enzyme resulting from environmental stress.

RESULTS

J20 Is a J-Protein That Delivers DXS to Plastidial Hsp70 Chaperones

Posttranscriptional regulation is a major factor determining the levels of active DXS, the first enzyme of the MEP pathway (Figure 1). To identify protein partners that could posttranslationally modulate DXS activity in *Arabidopsis*, we performed yeast two-hybrid screening. Among the possible DXS partners identified (see Supplemental Table 1 online), only four proteins were calculated to be interactors with high (category B) or very

high (category A) confidence. Of the three category B proteins, only one of them (At3g22970) might localize to plastids, but its function is unknown. Here, we report our work with the only category A protein identified, J20 (At4g13830), also named atDjC20 (Miernyk, 2001) and atDjC29 (Rajan and D'Silva, 2009). J20 is a plastid-localized J-protein that was proposed to contribute to photosynthetic efficiency (Chen et al., 2010) (see Supplemental Figure 1 online). The ability of J20 to bind to DXS was confirmed in vitro by pull-down assays (Figure 2A). Bimolecular fluorescence complementation experiments using leek (*Allium ampeloprasum*) epidermal cells further showed that, in plant cells, these two proteins interacted in plastids (see Supplemental Figure 2 online). To confirm that J20 and DXS were part of the same complex in *Arabidopsis*, we performed immunoprecipitation experiments using transgenic plants constitutively expressing a green fluorescent protein (GFP)–tagged version of J20 (*35S:J20-GFP* lines). Untransformed plants and transgenic lines expressing a GFP-fused DXR enzyme (as a control plastidial protein that does not interact with DXS) were also used for immunoprecipitation experiments with both anti-GFP and preimmune sera. DXS was detected only in *35S:J20-GFP* samples immunoprecipitated with the anti-GFP antibody, despite the very low level of J20-GFP protein detected in the input samples (Figure 2B). Taken together, these data show that J20 and DXS can efficiently interact in vivo.

Extensive work performed mainly in nonplant systems has previously demonstrated that J-proteins like J20 typically act as adaptors that recognize and deliver protein substrates to Hsp70, a molecular chaperone highly conserved in plants (Miernyk, 2001; Sung et al., 2001; Rajan and D'Silva, 2009; Kampinga and Craig, 2010). The J-domain responsible for the interaction with Hsp70 is well conserved in J20 (see Supplemental Figure 1 online), including the His-Pro-Asp tripeptide required for interaction with the chaperone (Wall et al., 1994; Tsai and Douglas, 1996). Upon interaction, ATP hydrolysis is stimulated to transfer the protein substrate to the Hsp70 chaperone and to drive conformational changes. To test the prediction that J20 might target DXS to the Hsp70 chaperone, transgenic *Arabidopsis* plants overexpressing a GFP-tagged DXS enzyme (*35S:DXS-GFP* lines) were used to immunoprecipitate DXS-containing complexes using an anti-GFP serum. Immunoblot analysis with an antibody specific for chloroplast Hsp70 proteins showed that these chaperones were indeed present in the immunoprecipitated samples (Figure 2C), confirming that DXS and Hsp70 can be found together in vivo.

Loss of Function of J20 Results in Decreased DXS Activity

To understand the biological relevance of the interaction of J20 with DXS, we next analyzed whether plants defective in J20 had any DXS-related phenotype. Changes in DXS activity cause altered sensitivity to clomazone (CLM), a specific DXS inhibitor (Zeidler et al., 2000; Carretero-Paulet et al., 2006; Matsue et al., 2010). In *Arabidopsis*, germination and growth in the presence of CLM result in concentration-dependent bleaching and a concomitant inhibition of true leaf development (Figure 3A), likely due to a reduced production of plastidial isoprenoid products, such as chlorophylls, carotenoids, and MEP-derived hormones (Figure 1). Plants with decreased DXS activity, such as the *dxs-3/chs5* mutant (Araki et al., 2000; Phillips et al., 2008), showed lower resistance to CLM
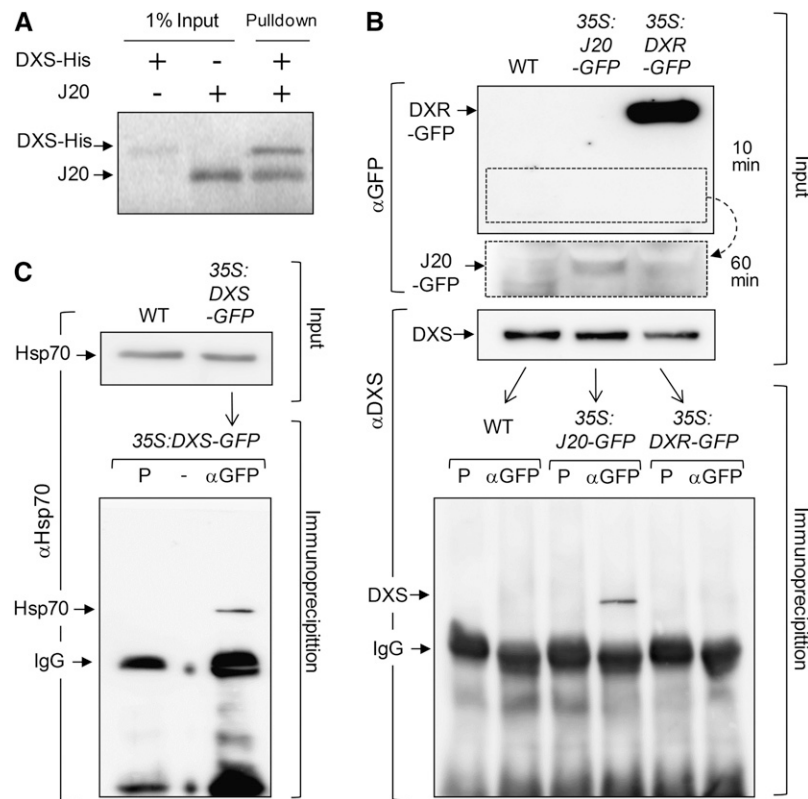
Figure 2. DXS Interacts with J20.

(A) In vitro pull-down assay using ³⁵S-labeled proteins DXS-His (immobilized on beads) and J20. Autoradiography of a SDS-PAGE gel loaded with the indicated samples before (input) and after the pull-down is shown.

(B) Immunoprecipitation of DXS from *35S:J20-GFP* plants expressing J20 fused to GFP. Protein extracts were obtained from *35S:J20-GFP* plants, control *35S:DXR-GFP* plants (producing another plastidial GFP-tagged protein, DXR-GFP) and wild-type (WT) plants. An aliquot (input) was used to test protein levels by immunoblot analysis using antibodies against GFP (αGFP) and DXS (αDXS). The same αGFP blot exposed for 10 and 60 min is shown to estimate the difference between the levels of J20-GFP (low) versus DXR-GFP (high). The rest of the extracts were used for immunoprecipitation experiments with either preimmune serum (P) or the commercial anti-GFP antibody. Immunoprecipitated samples were used for immunoblot analysis to detect the presence of the DXS protein. The position of the cross-reactive heavy chain of IgG is also indicated.

(C) Immunoblot analysis of samples obtained before (input) and after immunoprecipitation experiments using *35S:DXS-GFP* plants expressing DXS fused to GFP. Immunodetection was performed with an antibody specific for plastidial Hsp70 chaperones (αHsp70). The position of IgG is also marked.

(i.e., produced less chlorophyll when treated with the inhibitor) than the wild type, whereas DXS-overexpressing lines displayed reduced sensitivity to the inhibitor (see Supplemental Figure 3 online). Because a good correlation exists between CLM sensitivity and total DXS activity in *Arabidopsis* (see Supplemental Figure 3 online), we used this CLM assay to evaluate whether the loss of J20 function resulted in altered DXS activity. We first analyzed the Syngenta *Arabidopsis* Insertion Library line SAIL_1179_E04 harboring a T-DNA insertion in the first exon of *J20* (see Supplemental Figure 4A online), here referred to as *j20-1*. Wild-type and *j20-1* plants were germinated and grown on Murashige and Skoog (MS) plates supplemented with different concentrations of the inhibitor (Figure 3A). The visual phenotype of the *j20-1* mutant at a given concentration of CLM was similar to that of wild-type seedlings grown in the presence of higher concentrations of the inhibitor, indicating that the loss of J20 activity causes an increased sensitivity to CLM. Quantification of CLM sensitivity by measuring

chlorophyll levels in CLM-treated plants led to the same conclusion (Figure 3B; see Supplemental Figure 3 online). Measurement of DXS activity in wild-type and *j20-1* seedlings (Figure 4A) confirmed that the decreased CLM resistance phenotype of the mutant was caused by a substantial reduction in DXS activity (see Supplemental Figure 3 online). Because determining DXS activity in plant extracts is complicated, from this point we only used the CLM sensitivity assay to estimate DXS activity in vivo. Two independent lines of evidence confirmed that the phenotype of the *j20-1* mutant line was specifically caused by the loss of J20 activity. First, independent T-DNA insertion alleles from the Syngenta *Arabidopsis* Insertion Library and the Salk collections, herein referred to as *j20-2* (SAIL_569_H08) and *j20-3* (Salk_134365) (Chen et al., 2010), also showed CLM sensitivity (see Supplemental Figure 4A online). Second, transformation of *j20-1* plants with the *35S:J20-GFP* construct complemented the CLM sensitivity phenotype of the mutant (see Supplemental Figure 4B online).
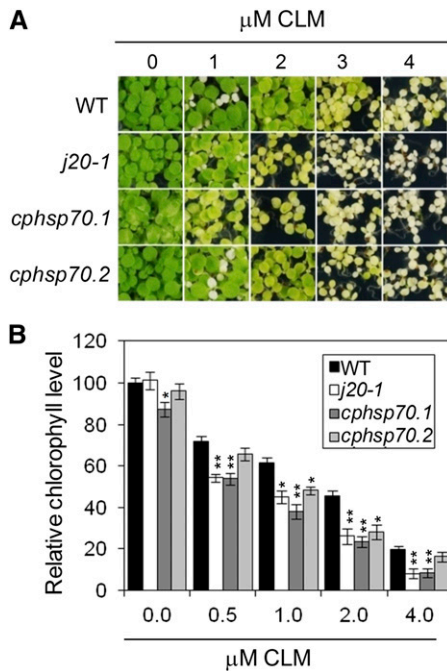
Figure 3. Mutants Defective in J20 or Individual Plastidial Hsp70 Chaperones Are Sensitive to CLM.

(A) Representative pictures of wild-type (WT) and *j20-1*, *cphsp70.1*, and *cphsp70.2* mutant plants germinated and grown for 10 d on MS medium containing the indicated concentrations of CLM.
(B) Total chlorophyll levels in samples like those shown in **(A)**. Data are represented relative to those in wild-type plants grown in the absence of CLM. Mean and SE values of $n \geq 5$ independent experiments are shown (Student's *t* test: *$P < 0.05$ and **$P < 0.01$).

There are more than 100 J-domain proteins in *Arabidopsis*, and several of them are targeted to plastids (Miernyk, 2001; Rajan and D'Silva, 2009; Chen et al., 2010). However, sequence analyses showed that J20 is more similar to J-proteins of other plant species than to the closest *Arabidopsis* J-domain proteins, J8, J11, and J41 (see Supplemental Figure 5A and Supplemental Data Set 1 online). *Arabidopsis* mutants impaired in J8 (At1g80920) or J11 (At4g36040) did not show the characteristic CLM sensitivity phenotype observed in J20-defective plants (see Supplemental Figure 5B online). Because the similarity between J20 and other plastidial J-proteins from *Arabidopsis*, including J8 and J11, is much lower at the C-terminal domain (see Supplemental Figure 1 online), which provides substrate specificity (Rajan and D'Silva, 2009), it is likely that this domain might confer specificity on J20, allowing it to interact with DXS to deliver the protein to the Hsp70 chaperone. Two plastidial (stromal) Hsp70 chaperones, cpHsp70.1 (At4g24280) and cpHsp70.2 (At5g49910), are found in *Arabidopsis* (Su and Li, 2008). If J20 and Hsp70 are part of the same mechanism regulating DXS activity, it should follow that mutants defective in plastidial Hsp70 activity also show a phenotype of higher sensitivity to CLM. Since mutants defective in both cpHsp70.1 and cpHsp70.2 are not viable (Su and Li, 2008), we analyzed single mutant lines. As shown in Figure 3, both single mutants showed a phenotype of increased CLM sensitivity relative to the wild type,

although this phenotype was stronger in the case of the *cphsp70.1* mutant. These results together demonstrate that loss of J20 function leads to reduced DXS activity (and, hence, CLM sensitivity) in vivo, most likely because it impairs targeting of this enzyme to the plastidial Hsp70 chaperone system.

Mutants Defective in J20 Show Posttranscriptional Accumulation of Inactive DXS in Chloroplasts

Hsp70 chaperones participate in protein import into organelles (including plastids), protein folding and assembly, and protein quality control. If J20 activity is required for the import of DXS into plastids, the decrease in enzyme activity observed in *j20-1* plants might be a result of reduced DXS protein levels in plastids. To address this possibility, DXS levels were analyzed in chloroplasts isolated from wild-type and mutant *j20-1* plants. Strikingly, immunoblot experiments with an anti-DXS antibody showed not decreased but increased levels of DXS protein in mutant chloroplasts (Figure 4B). This result suggests that loss of J20 function impairs processes occurring after the import of DXS, resulting in
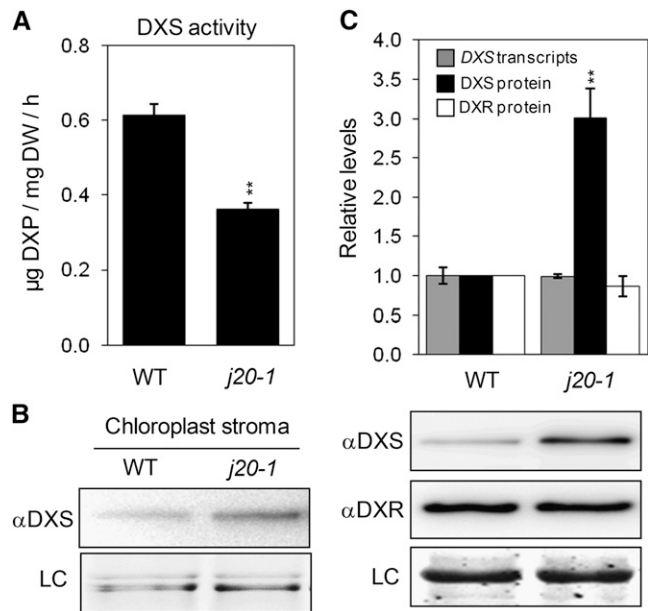

Figure 4. Loss of J20 Function Results in Lower DXS Activity but Higher Protein Levels.

(A) DXS activity levels in 10-d-old wild-type (WT) and mutant (*j20-1*) plants grown on MS plates. Values represent means and SE of $n = 3$ independent samples (Student's *t* test: **$P < 0.01$). DW, dry weight.
(B) Immunoblot analysis of DXS protein levels in chloroplasts isolated from wild-type and *j20-1* plants grown on MS plates for 2 weeks.
(C) Levels of DXS and DXR in samples like those described in **(A)**. RNA samples were used for quantitative PCR analysis of *DXS* transcript levels using the *APT1* gene as a normalizer. Protein samples extracted from the same plants were used for immunoblot analysis of DXS and DXR protein levels. The graph shows mean and SE values of $n \geq 3$ experiments (Student's *t* test: **$P < 0.01$). Representative images of immunoblot analyses and a Coomassie blue staining of the blots (loading control [LC]) are also shown.

the accumulation of inactive DXS protein in plastids. Consistent with this, the levels of DXS protein in total protein extracts of *j20-1* plants were threefold higher than those in the wild type without changes in the levels of DXS-encoding transcripts (Figure 4C). Although previous results have shown that posttranscriptional mechanisms regulating the accumulation of DXS protein can also affect the levels of DXR, the next enzyme of the MEP pathway (Guevara-García et al., 2005; Sauret-Güeto et al., 2006; Flores-Pérez et al., 2008), the amount of DXR protein detected in the same protein extracts showed no differences between mutant and wild-type plants (Figure 4C). In agreement with the presence of similar levels of DXR activity in wild-type and *j20-1* plants, no differences were observed in their sensitivity to the DXR-specific inhibitor fosmidomycin (see Supplemental Figure 4C online). These results suggest that J20 is not involved in regulating DXR levels or activity. Neither DXR nor DXS levels changed when the activity of close J20-related J-proteins, such as J8 or J11, was disrupted in mutants (see Supplemental Figure 5C online).

To provide additional experimental support to the conclusion that defective J20 activity results in posttranscriptional accumulation of inactive DXS protein inside chloroplasts, a transgenic *35S:DXS-GFP* line generated in the wild-type ecotype Columbia was selected to introgress the transgene into the *j20-1* background. After the cross, F3 siblings that were double homozygous for the transgene (based on marker gene resistance) and either the wild-type or the mutant *J20* gene (based on PCR-based genotyping) were selected. In agreement with the results described above, confocal laser scanning microscopy of GFP fluorescence showed that the DXS-GFP protein was localized to chloroplasts of siblings with either wild-type or mutant *J20* genes, but the levels were much higher in mutant plastids (Figure 5A). Interestingly, a spotted pattern of DXS-GFP fluorescence was observed in both types of siblings even though spots were much larger in the case of the mutant. This might be caused by the formation of DXS-GFP aggregates, although we cannot exclude other possibilities, such as the accumulation of the transgenic protein in subplastidial structures. Such aggregates (or structures) would most likely contain DXS in an inactive form because transgenic siblings of the *j20-1* background showed reduced resistance to CLM (Figure 5B) despite accumulating increased levels of constitutively expressed DXS-GFP protein (Figure 5C) compared with siblings with functional J20 protein.

J20 Might Promote the Degradation of Damaged DXS Proteins after Heat Stress

The results described above suggest that under normal growth conditions, J20 prevents the accumulation of inactive forms of DXS in chloroplasts. If the main role of J20 is to identify non-native DXS polypeptides and deliver them to Hsp70 for proper folding or refolding (i.e., enzyme activation), it could be expected that upregulating J20 levels would result in improved DXS activity. However, the presence of increasing levels of a functional GFP-tagged version of J20 (see Supplemental Figure 4B online) in different *35S:J20-GFP* lines led to reduced DXS levels and a bleached phenotype (Figure 6A; see Supplemental Table 2 online). Transgenic lines with highest J20-GFP levels showed an albino phenotype similar to that of the DXS-defective *dxs-1/cla1*

mutant (Mandel et al., 1996; Estévez et al., 2000; Phillips et al., 2008). Despite this dramatic phenotypic effect, no major changes in the levels of other proteins like DXR or Hsp70 isoforms were detected in *35S:J20-GFP* lines relative to wild-type (untransformed) or mutant *dxs-1/cla1* plants (Figure 6A). These results suggest that abnormally high levels of J20 prevent the accumulation of DXS polypeptides without altering the levels of other plastidial proteins.

To evaluate whether J20 might contribute to degrade DXS polypeptides that could be damaged (misfolded) following environmental stress, plants growing at 22°C were transferred to 45°C and samples were collected at different times after the heat shock for immunoblot analysis of DXS protein levels. As shown in Figure 6B, DXS was rapidly degraded after the heat shock in the wild type, whereas the degradation rate was slower in mutant plants. By contrast, DXR was more stable after a heat shock and its levels remained similar in wild-type and *j20-1* plants (Figure 6C). The levels of plastidial Hsp70 proteins also remained unchanged in wild-type and mutant plants during this period (Figure 6D), supporting the conclusion that the rate of DXS degradation depends on the levels of J20 but not of Hsp70 chaperones. Together, our data suggest that J20 (via Hsp70) might promote degradation of DXS proteins that are damaged (misfolded) and, hence, inactivated after a heat stress episode.

DISCUSSION

Plastids provide fundamental and unique biochemical pathways for plant cells, including the essential MEP pathway for the production of isoprenoids required for photosynthesis, photoprotection, and plant development. It is widely accepted that plastids, like mitochondria, were acquired by a symbiosis between the ancestors of eukaryotic cells and prokaryotic organisms early during evolution. However, they still remain as separate functional entities that regulate their own biochemistry in a relatively independent way. An important part of this regulation deals with the control of enzyme activities inside plastids. Most enzymes participating in plastidial metabolism, including those of the MEP pathway, are encoded by nuclear genes, synthesized in precursor form in the cytosol, and transported into plastids using intricate energy-dependent import machineries assisted by Hsp70 and several other chaperones and cochaperones (Rodríguez-Concepción and Boronat, 2002; Shi and Theg, 2010; Su and Li, 2010; Flores-Pérez and Jarvis, 2013). Upon import and arrival in the stroma, plastidial Hsp70 chaperones also appear to contribute to the folding, assembly, or onward intraorganellar guidance of these plastid-targeted proteins (Yalovsky et al., 1992; Madueño et al., 1993; Tsugeki and Nishimura, 1993; Liu et al., 2007; Nordhues et al., 2010). Once in their final, active form, the enzymes must be maintained in a functional state despite multiple stresses. This process, referred to as protein quality control, involves different mechanisms to deal with damaged (misfolded) proteins either by stabilization, refolding, or degradation. Misfolding in the chloroplast context can be caused by metabolic perturbation or environmental stress, such as excess light, temperature peaks, etc. (Wickner et al., 1999; Huang et al., 2001). Hsp70 chaperones
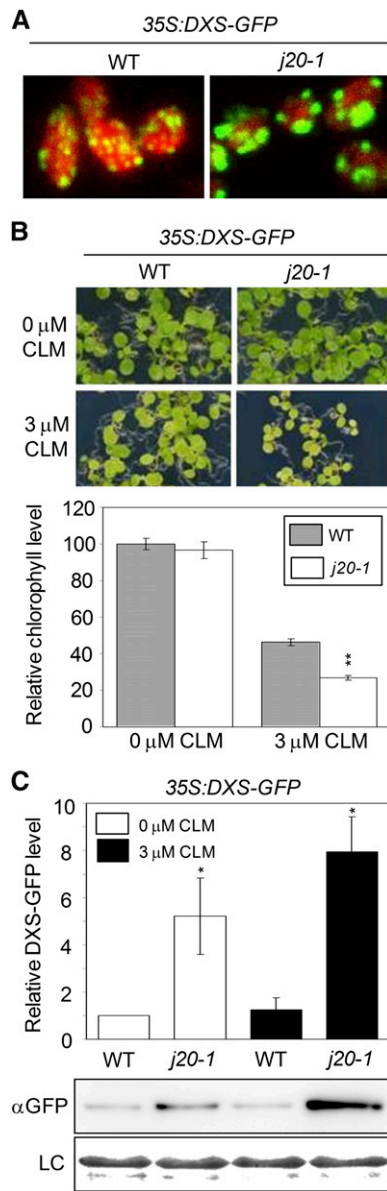
Figure 5. Defective J20 Activity Results in Posttranscriptional Accumulation of Inactive DXS Protein in Chloroplasts.

(A) Confocal microscopy detection of GFP (green) and chlorophyll (red) fluorescence in chloroplasts of siblings harboring the same T-DNA insertion with the *35S:DXS-GFP* construct in a wild-type (WT) or J20-defective (*j20-1*) background. The images were obtained with the same confocal parameters.
(B) CLM resistance of the transgenic *35S:DXS-GFP* lines described in **(A)**. Plants were germinated and grown for 10 d on MS either supplemented or not with 3 μM CLM. The bottom panel shows the quantification of CLM resistance represented as the levels of chlorophylls in the plants shown in the top panels. Data are represented relative to those in plants with a wild-type *J20* gene grown without CLM. Mean and SE values of *n* = 3 independent experiments are shown (Student's *t* test: **P < 0.01).
(C) Immunoblot analysis of DXS-GFP levels in the samples described in **(B)**. The graph shows mean and SE values of *n* = 3 experiments

prevent aggregation of misfolded proteins and, together with other chaperones, promote the solubilization of toxic protein aggregates. Additionally, Hsp70 chaperones facilitate the transfer of client proteins to proteolytic systems (Hayes and Dice, 1996; Lee et al., 2009; Kampinga and Craig, 2010; Nordhues et al., 2010; Voos, 2013).

The specificity of Hsp70 chaperones to function in distinct processes is determined by their partner J-proteins, which act as adaptors that recognize particular substrates and transfer them to the chaperone. Most organisms typically contain a few Hsp70 isoforms but a much higher number of J-proteins in different cell compartments. For example, the *Arabidopsis* genome contains 14 genes encoding Hsp70 chaperones (two of them plastidial) but more than 100 genes encoding J-proteins, including several plastidial isoforms (Lin et al., 2001; Miernyk, 2001; Ratnayake et al., 2008; Su and Li, 2008; Rajan and D'Silva, 2009; Chen et al., 2010). Thus, it is expected that one Hsp70 interacts with different J-proteins to perform specific functions. Based on emerging research, it was concluded that chloroplast-localized J-proteins might assist in the folding/unfolding and assembly/disassembly of proteins involved in processes such as photosynthetic efficiency (Chen et al., 2010), thylakoid biogenesis (Liu et al., 2007; Tanz et al., 2012), chloroplast division (Vitha et al., 2003), and chromoplast differentiation (Lu et al., 2006). However, the client proteins and physiological roles of most plastidic J-proteins remain largely unknown. Here, we report that the plastidial J-protein J20 interacts with DXS, the first enzyme of the MEP pathway, and delivers it to the Hsp70 chaperone. J20 has a unique substrate binding C-terminal domain (see Supplemental Figure 1 online) and belongs to a class of J-proteins (class III) that typically bind one or a few proteins (Craig et al., 2006; Rajan and D'Silva, 2009). Analysis of mutant plants defective in J20 and two other similar plastidial proteins (J8 and J11) led to the proposal of a role for these J-proteins in optimization of photosynthesis, redox regulation, and tolerance to oxidative stress (Chen et al., 2010). In addition to playing partially redundant roles, it was concluded that each protein also had specific functions. In particular, J11 and J20 were proposed to have a predominant role in the stabilization of photosynthetic pigment-protein complexes of photosystem II. The stability of such complexes was found to be lower in the mutants after exposure to high light, and the same was observed for photosystem II dimers. Additionally, mutants accumulated lower levels of ribulose-1,5-bis-phosphate carboxylase/oxygenase activase when grown in the light, suggesting a possible role of these J-proteins in the folding or assembly of the enzyme (Chen et al., 2010). However, no evidence of direct physical interaction with any client protein was provided. Here, we demonstrate that defects in the activity of J20, but not J8 or J11, cause enhanced accumulation of inactive DXS polypeptides but reduced DXS activity. The decrease in DXS activity observed in J20-defective mutants might result in lower levels of MEP-derived isoprenoids relevant for photosynthesis under some environmental

(Student's *t* test: *P < 0.05). Representative images of a blot decorated with anti-GFP serum and stained with Coomassie blue (loading control [LC]) are also shown.
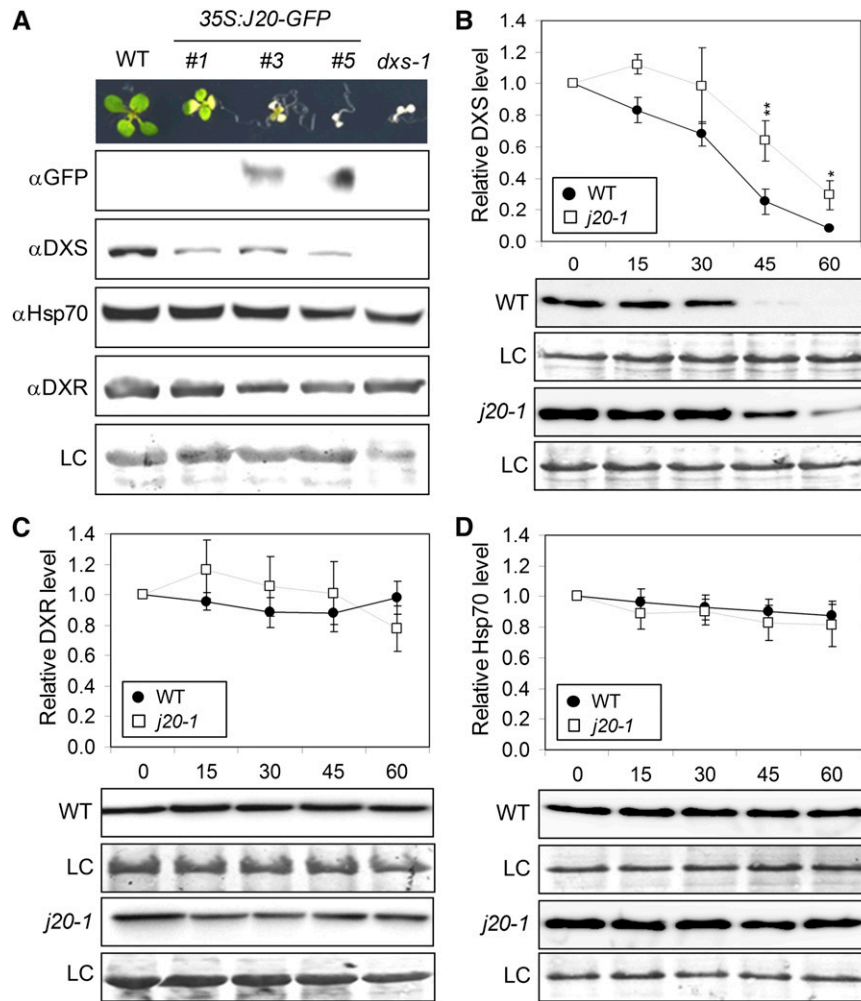
Figure 6. J20 Promotes Degradation of DXS after a Heat Shock.

(A) Phenotype of 2-week-old plants from different *35S:J20-GFP* lines compared with the wild-type (WT) and a DXS-deficient (*dxs-1*) mutant. Representative images of immunoblot analyses of J20-GFP, DXS, plastidial Hsp70, and DXR protein levels in these plants, as well as a Coomassie blue staining of the blots (loading control [LC]), are also shown.

(B) to **(D)** Immunoblot analysis of DXS **(B)**, DXR **(C)**, and plastidial Hsp70 **(D)** protein levels after a heat shock. Wild-type and mutant *j20-1* plants grown for 10 d at 22°C were transferred to 45°C and samples were collected after the indicated times (min, *x* axis). Representative blots and quantitative data corresponding to the mean and SE values of $n \geq 6$ independent experiments are shown (Student's *t* test: *$P < 0.05$ and **$P < 0.01$).
[See online article for color version of this figure.]

conditions, such as high light. This could lead to some of the phenotypes previously described for the mutant, including the limited photosynthetic performance (Chen et al., 2010). However, we cannot exclude that J20 might participate in other processes unrelated to the MEP pathway that could explain the redundant functions with J8 and J11.

Based on the experimental evidence reported here, we propose the model represented in Figure 7. Under normal growth conditions, J20 might recognize DXS polypeptides that remain unfolded after plastid import or become misfolded upon ordinary perturbations, transferring them to Hsp70 chaperones for refolding and, hence, enzyme activation. In response to more severe conditions (such as heat shock), DXS polypeptides might be

prone to rapid misfolding or denaturation, overwhelming the capacity of the J20/Hsp70 system to repair them. In this context, J20 might target inactive DXS enzymes for proteolytic removal (Figure 7). It is likely that an abnormal increase in J20 activity in transgenic *35S:J20-GFP* plants might also result in an increased degradation rate of DXS even under optimal growth conditions, eventually resulting in reduced levels of the enzyme (Figure 6; see Supplemental Table 2 online). The fact that DXS polypeptides were still detected in plants with the strongest J20-GFP accumulation suggests that a portion of DXS would not be degraded but it might remain associated with the chimeric J-protein, hence preventing enzyme activity. This possibility would explain the bleached phenotype of the *35S:J20-GFP* plants (the expected

consequence of a block in the MEP pathway) as well as the efficient recovery of DXS protein in coimmunoprecipitation experiments despite the presence of low levels of J20-GFP protein in the transgenic lines (Figure 2B). Alternatively, an additional role of J20 in maintaining normal photosynthetic activity (Chen et al., 2010) might also explain why increased levels cause bleaching.

A role for cytosolic J-proteins and Hsp70 chaperones in mediating degradation of client proteins has been reported in plants. For example, the delivery of viral coat proteins to Hsp70 mediated by the cytosolic J-protein CPIP promotes their degradation by increasing their ubiquitination (Hafrén et al., 2010). Cytosolic Hsp70 also appears to be involved in the ubiquitination and degradation of plastid-targeted preproteins when chloroplast import is defective (Lee et al., 2009). However, plastids lack the ubiquitin/proteasome pathway and rely in other proteolytic machineries for protein removal, including protease systems of bacterial origin, such as Clp, Lon, FtsH, and Deg (Kato and Sakamoto, 2010). The question of what protease(s) could be involved in the specific J20-mediated degradation of DXS in plastids remains open at the moment. Increased levels of DXS, DXR, and other MEP pathway

enzymes were found in mutants with decreased activity of the stromal Clp protease complex (Flores-Pérez et al., 2008; Kim et al., 2009; Zybailov et al., 2009). However, several proteases could be involved in the proteolytic removal of DXS, as reported for the plastidial D1 protein, which is degraded by FtsH and Deg proteases (Kato et al., 2012). Consistent with this, bacterial Hsp70 assists in the degradation of unfolded proteins mediated by FtsH (Rodriguez et al., 2008) and Lon (Sakr et al., 2010) proteases.

Understanding how plants regulate their plastidial metabolism under normal growth conditions but also in response to environmental challenges, such as temperature stress, is of both basic and applied importance. Interestingly, the ~50% decrease in DXS activity measured in J20-defective plants (Figure 4A) did not have an effect on the production of chlorophylls (Figure 3B) or the visual phenotype of *j20-1* (Figure 3A; see Supplemental Figure 4 online) or *j20-3* (Chen et al., 2010) mutants compared with wild-type plants grown under normal conditions. This is consistent with the lack of phenotypic changes observed in heterozygous individuals for the knockout *dxs-1/cla1* mutation (which have a 50% reduction in the no. of functional DXS copies) or transgenic lines with antisense-mediated reduction of DXS levels relative to wild-type siblings (Mandel et al., 1996; Estévez et al., 2001). A reduction of DXS activity levels was also observed in the knockdown *dxs-3/chs5* mutant (see Supplemental Figure 3 online), which displays a wild-type phenotype when grown under normal conditions and shows bleaching only when transferred to restrictive temperatures (Araki et al., 2000; Phillips et al., 2008). It is therefore likely that a strong reduction in DXS activity does not compromise growth of *Arabidopsis* plants under optimal conditions, but it may be relevant in response to stress (like temperature changes). Indeed, the high susceptibility of DXS to proteolytic degradation after a heat shock (Figure 6B) might have a regulatory function for isoprenoid biosynthesis. To date, the overexpression of DXS and other enzymes of the MEP pathway has been only partially successful in increasing the production of plastidial isoprenoids of interest, in part because posttranscriptional regulation might prevent substantial increases in enzyme activities. The activity of MEP pathway enzymes has been found to be modulated by feedback regulation by pathway intermediates, phosphorylation, redox control, and, as supported by our data, proteolytic degradation in the plastid (Rodríguez-Concepción, 2006; Cordoba et al., 2009; Hemmerlin, 2013). The work reported here further implicates a J-protein (J20) and Hsp70 chaperones in the posttranscriptional regulation of DXS activity. The plastidial Hsp70 system appears to contribute to the regulation of MEP-derived isoprenoid biosynthesis in several steps. For example, the cauliflower (*Brassica oleracea*) *orange* mutation was mapped to a gene encoding a plastidial J-protein presumably involved in the differentiation of chromoplasts and the biosynthesis of carotenoids (Lu et al., 2006), and carotenoid biosynthetic enzymes were found in Hsp70-containing complexes in *Narcissus pseudonarcissus* chromoplasts (Al-Babili et al., 1996; Bonk et al., 1996). More knowledge of how protein quality control systems regulate enzyme activity in plastids should inform decisions in future biotechnological approaches aimed at manipulating the levels of plastidial metabolites in crop plants.
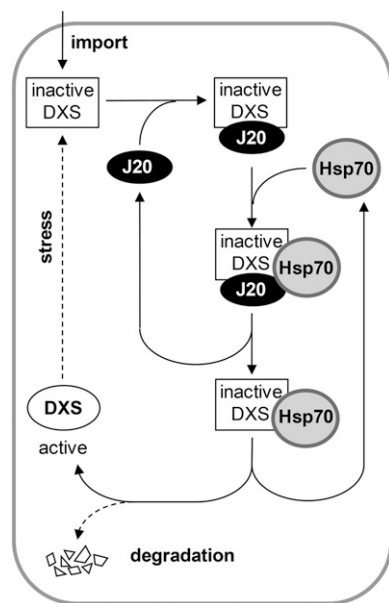

Figure 7. A Model for the Contribution of J20 and Hsp70 Chaperones to Modulating the Levels of Active DXS Enzymes.

The mode of action of J20 and plastidial Hsp70 chaperones is based on previous J-protein/Hsp70 models basically developed from in vitro refolding studies of denatured proteins (Rajan and D'Silva, 2009; Kampinga and Craig, 2010). The rest of the model is based on the data reported in this work. J20 might normally recognize inactive DXS polypeptides that remain unfolded after plastid import or become misfolded upon ordinary perturbations, transferring them to Hsp70 chaperones for refolding and, hence, enzyme activation. Upon heat shock or other severe stress, active DXS polypeptides might undergo rapid misfolding or denaturation and overwhelm the repair capacity of the J20/Hsp70 system. In this context, J20 might target inactive DXS enzymes for proteolytic degradation.

METHODS

Plant Material and Growth Conditions

All *Arabidopsis thaliana* lines used in this work are in the Columbia background. Seeds from *cphsp70.1* and *cphsp70.2* (Su and Li, 2008) were kindly provided by Hsou-min Li (Academia Sinica, Taiwan), whereas those from *j20-3*, *j8*, and *j11* mutants (Chen et al., 2010) were kindly provided by Eva-Mari Aro (University of Turku, Finland). The T-DNA insertion lines SAIL_1179_E04 (*j20-1*) and SAIL_569_H08 (*j20-2*) were obtained from the European Stock Centre. For the generation of transgenic plants, full-length cDNAs encoding *Arabidopsis* DXS or DXR were cloned into plasmid pB7FWG2 (Karimi et al., 2002) and J20 into pCAMBIA1302, respectively. Constructs and primers are described in detail in Supplemental Tables 3 and 4 online. The constructs, encoding the chimeric proteins DXS-GFP, DXR-GFP, and J20-GFP under the control of the constitutive *35S* promoter, were used for *Agrobacterium tumefaciens*–mediated transformation of *Arabidopsis* plants. Homozygous lines containing a single T-DNA insertion were selected based on the segregation of the resistance marker (glufosinate or hygromycin, respectively). Seeds were surface-sterilized and germinated in Petri dishes with solid MS medium. When indicated, plates were supplemented with the indicated concentrations of CLM or fosmidomycin. After stratification for 3 d at 4°C, plates were incubated in a growth chamber at 22°C under long days (8 h in darkness and 16 h under fluorescent white light at a PPFD of 60 μmol m^{-2} s^{-1}). Heat stress experiments were performed by directly transferring plates with 10-d-old seedlings from 22 to 45°C.

Protein–Protein Interaction Analyses

The yeast two-hybrid screen was performed by Hybrigenics using the *Arabidopsis* RP1 library (see Supplemental Table 1 online). A recombinant *Arabidopsis* DXS protein lacking the transit peptide and fused to a C-terminal 6xHis-tag (from clone pET-DXS-His; see Supplemental Table 3 online) was used as a bait (N-LexA-ΔPTDXS-C fusion). The in vitro pull-down assay was performed following a previously described protocol (Ni et al., 1999). Briefly, constructs pET-DXS-His and pBS-J20 (see Supplemental Table 3 online) were used to synthesize ^{35}S-labeled proteins with the TnT system (Promega). The DXS-His protein was bound to agarose beads and incubated with precleared J20 TnT mix maintaining roughly the same amounts of labeled DXS-His and J20 protein. Following incubation at 4°C for 4 h, agarose beads were pelleted and washed, and the attached proteins were separated and analyzed by SDS-PAGE. The gel was dried and exposed to a phosphor imager screen. For bimolecular fluorescence complementation experiments, cDNA sequences encoding full-length DXS and J20 proteins were cloned in appropriate vectors (Ohad et al., 2007) (see Supplemental Table 3 online). Leek (*Allium ampeloprasum*) epidermal peels were microbombarded with DNA-coated 1 μM gold microcarriers using a Biolistic PDS-1000/He system (Bio-Rad) and incubated at 22°C in the dark for 24 h prior to observation with a Leica TCS 4D confocal laser scanning microscope.

Protein Extraction, Immunoblot Analysis, and Immunoprecipitation

Whole plants or chloroplasts isolated as described (Flores-Pérez et al., 2008) were used for protein extraction and immunoblot analysis using antibodies against *Arabidopsis* DXS (developed against the recombinant protein from construct pET-DXS-His by Abyntek), maize (*Zea mays*) DXR (Hans et al. 2004) (a kind gift of Michael H. Walter, Leibniz Institute of Plant Biochemistry), chloroplast Hsp70 (Agrisera), or GFP (Invitrogen). The preimmune serum was isolated from rabbits used for the production of the DXS antibody (Abyntek). Total plant protein extracts were obtained from 50 mg of fresh tissue by grinding samples in liquid nitrogen. The powder was resuspended in 100 μL of ice-cold TKMES homogenization buffer (100 mM

Tricine-potassium hydroxide, pH 7.5, 10 mM KCl, 1 mM MgCl$_2$, 1 mM EDTA, and 10% [w/v] Suc) supplemented with 0.2% (v/v) Triton X-100, 1 mM DTT, 100 μg/mL phenylmethylsulfonyl fluoride, 3 μg/mL E64, and 20 μL/mL protease inhibitor cocktail (Sigma-Aldrich). The resuspended sample was centrifuged at 2300g for 10 min at 4°C and the supernatant recovered for a second step of centrifugation. Supernatant protein concentration was determined using the Bio-Rad protein assay. After SDS-PAGE, the proteins were electrotransferred to Hybond-P polyvinylidene difluoride membranes (Amersham) as described (Rodríguez-Concepción et al., 2001). After the protein transfer was completed, membranes were incubated overnight at 4°C with the corresponding primary antibody (diluted 1:500 for DXS, 1:6000 for DXR, 1:6000 for Hsp70, and 1:2000 for GFP). Incubation with the horseradish peroxidase–conjugated secondary antibody (diluted 1:10,000) was performed for 30 min at room temperature. Detection of immunoreactive bands was performed using the ECL Plus reagent (Amersham). Chemiluminescent signals were visualized using a LAS-4000 image analyzer (Fujifilm) and quantified with Quantity One (Bio-Rad). Student's t test was used to assess statistical significance of quantified differences.

For immunoprecipitation experiments, ~4 g of tissue from 2-week-old plants was ground in liquid nitrogen and incubated in RIPA buffer (50 mM Tris-HCl, pH 8, 150 mM NaCl, 1% [w/v] Nonidet P-40, and 0.1% [w/v] SDS) for 30 min at 4°C on a rotating platform. After centrifugation at 14,000g for 30 min at 4°C, supernatant was filtered through Miracloth (Calbiochem) twice and mixed with Sepharose beads containing the appropriate antibody, previously prepared by overnight incubation of 5 μL of antibody and 100 μL of Sepharose beads (Healthcare) in 10 mM sodium phosphate, pH 7, 150 mM NaCl, and 10 mM EDTA. After incubation for 4 h at 4°C, the mixture was centrifuged (3000g, 2 min, 4°C) and the pellet washed four to five times with RIPA buffer without detergents. To visualize the protein complexes bound to the antibody in the washed beads, 100 μL of protein loading buffer was added to the last pellet and the mixture was analyzed by SDS-PAGE and immunoblot.

RNA Isolation and Quantitative PCR Analysis

Total RNA was isolated using a RNA purification kit (Sigma-Aldrich) and reverse-transcribed using SuperScript II (Invitrogen). The quantitative PCR experiments were performed as described (Rodríguez-Villalón et al., 2009) using Fast Start Universal SYBR Green Master Mix (Roche) on a Light Cycler 480 apparatus (Roche). The *APT1* (At1g27450) gene was used for normalization. Primer sequences for quantitative PCR reactions are listed in Supplemental Table 4 online.

DXS Enzyme Activity and Chlorophyll Determination

DXS enzyme activity was measured in 10-d-old seedlings grown on MS plates. Whole seedlings were ground in liquid nitrogen and lyophilized overnight. Lyophilized tissue (5 mg) was extracted in 1 mL of extraction buffer at 4°C containing 50 mM Tris-HCl, pH 8.0, 10% (v/v) glycerol, 0.5% (v/v) Tween 20, 1% (w/v) polyvinylpolypyrrolidone (average molecular weight = 360,000), 100 μM thiamin pyrophosphate, 10 mM DTT, 1 mM ascorbate, 2 mM imidazole, 1 mM sodium fluoride, 1.15 mM sodium molybdate, and 1% protease inhibitor cocktail (Sigma-Aldrich). Extracts were gently mixed at 4°C for 15 min on a rotating wheel, followed by centrifugation at 20,000g for 20 min. A 30-μL aliquot of each supernatant was mixed with 70 μL of enzyme reaction buffer and incubated for 2 h at 30°C. The reaction buffer for DXS activity contained 50 mM Tris-HCl, pH 8.5, 10 mM MgCl$_2$, 10% (v/v) glycerol, 2,5 mM DTT, 1 mM thiamin pyrophosphate, 10 mM pyruvate, 10 mM glyceraldehyde 3-phosphate, 2 mM imidazole, 1 mM sodium fluoride, 1.15 mM sodium molybdate, and 1% protease inhibitor cocktail. After incubation, 100 μL of chloroform was added to each reaction, and the tubes were vigorously vortexed. The mixture was centrifuged at 13,000g for 5 min, and 45 μL of the aqueous

(upper) phase was transferred to an liquid chromatography vial containing 5 μL [1,2,3-$^{13}C_3$]DXP at 10 ng/μL. The product of DXS (DXP) was separated using a 1200 series liquid chromatograph (Agilent Technologies) as follows. A 20-μL aliquot of the reaction mixture was injected onto a Nucleodex β-OH column (5 μm, 200 × 4 mm; Macherey-Nagel) with a guard column containing the same sorbent equilibrated at 10% solvent A (10 mM ammonium acetate) and 90% solvent B (acetonitrile). After 5 min of isocratic separation at 10% solvent A, a gradient was initiated, leading to 50% solvent A by 15 min, followed by a wash step with 50% solvent A for 5 min and return to initial conditions and 10 min of further equilibration. Mass selective detection of the eluent was performed using a connected API 3200 triple quadrupole mass spectrometer (Applied Biosystems) operating in negative ionization mode with the following instrument settings: ion spray voltage of −4200 eV, turbo gas temperature of 700°C, nebulizer gas at 70 p.s.i., heating gas at 70 p.s.i., curtain gas at 20 p.s.i., and collision gas at 5 p.s.i. Multiple reaction monitoring was used to monitor analyte precursor ion → quantifier ion: mass-to-charge ratio (m/z) of 212.9 → 78.9 for enzymatically produced DXP and m/z 215.9 → 78.9 for the isotopic labeled $^{13}C_3$ DXP internal standard (collision energy of −42 V, declustering potential of −20 V, and entrance potential of −7 V). Both Q1 and Q2 quadrupoles were maintained at unit resolution. Analyst 1.5 software (Applied Biosystems) was used for data acquisition and processing. DXS activity measured in this way was normalized to the mass of tissue used in the protein extract. Quantification was accomplished by comparing the integrated peak area to that of an external standard curve composed of authentic DXP ranging from 0.1 to 10 ng/μL. This amount was normalized to the coeluting peak of [1,2,3-$^{13}C_3$]DXP (detected at m/z 215.9) to correct for ion suppression effects. Unlabeled DXP standard was obtained from Sigma-Aldrich, and [1,2,3-$^{13}C_3$]DXP was a kind gift from Wolfgang Eisenreich. Photosynthetic pigments were extracted with 80% (v/v) ice-cold acetone from 50 mg of fresh tissue (whole plants). Chlorophyll determinations were performed as described (Lichtenthaler and Wellburn, 1983).

Phylogenetic Analysis

Sequences were retrieved using the C-terminal domain of *Arabidopsis* J8, J11, J20, and J41 as queries in BLAST searches on the National Center for Biotechnology Information webpage (www.ncbi.nlm.nih.gov/). Sequences lacking the transit peptides predicted with TargetP (www.cbs.dtu.dk/services/TargetP) were aligned with Clustal Omega (www.ebi.ac.uk/Tools/msa/clustalo/) (see Supplemental Data Set 1 online), and a phylogenetic tree rooted at midpoint was constructed using the neighbor-joining method in MEGA5 (megasoftware.net/). The evolutionary distances were computed using the Poisson correction method, and the bootstrap test was selected with 2000 replications.

Accession Numbers

Sequence data from this article can be found in the Arabidopsis Genome Initiative or GenBank/EMBL databases under the following accession numbers: J8, At1g80920; J11, At4g36040; J20, At4g13830; J41, At2g17880; cpHsp70.1, At4g24280; cpHsp70.2, At5g49910; DXR, At5g62790; and DXS, At4g15560. Yeast two-hybrid results were submitted to The International Molecular Exchange Consortium (http://www.imexconsortium.org) through IntAct (http://www.ebi.ac.uk/intact/) and assigned the identifier IM-20956.

Supplemental Data

The following materials are available in the online version of this article.

Supplemental Figure 1. *Arabidopsis* J20 Is a J-Protein.

Supplemental Figure 2. BiFC Experiments Using Leek Epidermal Cells.

Supplemental Figure 3. Validation of the CLM Resistance Assay as a Good Estimate of DXS Activity Levels.

Supplemental Figure 4. Sensitivity of Mutant and Transgenic Lines to Specific DXS and DXR Inhibitors.

Supplemental Figure 5. *Arabidopsis* Mutants Defective in J20-Related J-Proteins Do Not Show a CLM Sensitivity Phenotype.

Supplemental Table 1. Summary of Results from the Yeast Two-Hybrid Screen.

Supplemental Table 2. Quantification of DXS Protein Levels in *35S*:*J20-GFP* Lines.

Supplemental Table 3. Constructs and Cloning Details.

Supplemental Table 4. Primers Used in This Work.

Supplemental Data Set 1. Text File of the Alignment Used to Generate the Phylogenetic Tree Shown in Supplemental Figure 5A.

AUTHOR CONTRIBUTIONS

P.P. and M.R.-C. conceived the project and designed the research. P.P., G.T.-O., M.A.P., and L.P.W. performed the experimental work and contributed new analytic tools. P.P., G.T.O., M.A.P., L.P.W., and M.R.-C. analyzed the results and provided input for discussion. P.P. and M.R.-C. wrote the article.

REFERENCES

Al-Babili, S., von Lintig, J., Haubruck, H., and Beyer, P. (1996). A novel, soluble form of phytoene desaturase from *Narcissus pseudonarcissus* chromoplasts is Hsp70-complexed and competent for flavinylation, membrane association and enzymatic activation. Plant J. **9:** 601–612.

Araki, N., Kusumi, K., Masamoto, K., Niwa, Y., and Iba, K. (2000). Temperature -sensitive *Arabidopsis* mutant defective in 1-deoxy-D-xylulose 5-phosphate synthase within the plastid non-mevalonate pathway of isoprenoid biosynthesis. Physiol. Plant. **108:** 19–24.

Bonk, M., Tadros, M., Vandekerckhove, J., Al-Babili, S., and Beyer, P. (1996). Purification and characterization of chaperonin 60 and heat-shock protein 70 from chromoplasts of *Narcissus pseudonarcissus*. Plant Physiol. **111:** 931–939.

Boston, R.S., Viitanen, P.V., and Vierling, E. (1996). Molecular chaperones and protein folding in plants. Plant Mol. Biol. **32:** 191–222.

Botella-Pavía, P., and Rodríguez-Concepción, M. (2006). Carotenoid biotechnology in plants for nutritionally improved foods. Physiol. Plant. **126:** 369–381.

Carretero-Paulet, L., Ahumada, I., Cunillera, N., Rodríguez-Concepción, M., Ferrer, A., Boronat, A., and Campos, N. (2002). Expression and molecular analysis of the Arabidopsis DXR gene encoding 1-deoxy-D-xylulose 5-phosphate reductoisomerase, the first committed enzyme of the 2-C-methyl-D-erythritol 4-phosphate pathway. Plant Physiol. **129:** 1581–1591.

Carretero-Paulet, L., Cairó, A., Botella-Pavía, P., Besumbes, O., Campos, N., Boronat, A., and Rodríguez-Concepción, M. (2006). Enhanced flux through the methylerythritol 4-phosphate pathway in *Arabidopsis* plants overexpressing deoxyxylulose 5-phosphate reductoisomerase. Plant Mol. Biol. **62:** 683–695.

Chen, K.M., Holmström, M., Raksajit, W., Suorsa, M., Piippo, M., and Aro, E.M. (2010). Small chloroplast-targeted DnaJ proteins are involved in optimization of photosynthetic reactions in *Arabidopsis thaliana*. BMC Plant Biol. **10:** 43.

Cordoba, E., Salmi, M., and León, P. (2009). Unravelling the regulatory mechanisms that modulate the MEP pathway in higher plants. J. Exp. Bot. **60:** 2933–2943.

Craig, E.A., Huang, P., Aron, R., and Andrew, A. (2006). The diverse roles of J-proteins, the obligate Hsp70 co-chaperone. Rev. Physiol. Biochem. Pharmacol. **156:** 1–21.

DellaPenna, D., and Pogson, B.J. (2006). Vitamin synthesis in plants: Tocopherols and carotenoids. Annu. Rev. Plant Biol. **57:** 711–738.

Enfissi, E.M.A., Fraser, P.D., Lois, L.M., Boronat, A., Schuch, W., and Bramley, P.M. (2005). Metabolic engineering of the mevalonate and non-mevalonate isopentenyl diphosphate-forming pathways for the production of health-promoting isoprenoids in tomato. Plant Biotechnol. J. **3:** 17–27.

Estévez, J.M., Cantero, A., Reindl, A., Reichler, S., and León, P. (2001). 1-Deoxy-D-xylulose-5-phosphate synthase, a limiting enzyme for plastidic isoprenoid biosynthesis in plants. J. Biol. Chem. **276:** 22901–22909.

Estévez, J.M., Cantero, A., Romero, C., Kawaide, H., Jiménez, L.F., Kuzuyama, T., Seto, H., Kamiya, Y., and León, P. (2000). Analysis of the expression of CLA1, a gene that encodes the 1-deoxyxylulose 5-phosphate synthase of the 2-C-methyl-D-erythritol-4-phosphate pathway in Arabidopsis. Plant Physiol. **124:** 95–104.

Flores-Pérez, U., and Jarvis, P. (2013). Molecular chaperone involvement in chloroplast protein import. Biochim. Biophys. Acta **1833:** 332–340.

Flores-Pérez, U., Pérez-Gil, J., Closa, M., Wright, L.P., Botella-Pavía, P., Phillips, M.A., Ferrer, A., Gershenzon, J., and Rodríguez-Concepción, M. (2010). Pleiotropic regulatory locus 1 (PRL1) integrates the regulation of sugar responses with isoprenoid metabolism in *Arabidopsis*. Mol. Plant **3:** 101–112.

Flores-Pérez, U., Sauret-Güeto, S., Gas, E., Jarvis, P., and Rodríguez-Concepción, M. (2008). A mutant impaired in the production of plastome-encoded proteins uncovers a mechanism for the homeostasis of isoprenoid biosynthetic enzymes in *Arabidopsis* plastids. Plant Cell **20:** 1303–1315.

Guevara-García, A., San Román, C., Arroyo, A., Cortés, M.E., de la Luz Gutiérrez-Nava, M., and León, P. (2005). Characterization of the *Arabidopsis* clb6 mutant illustrates the importance of posttranscriptional regulation of the methyl-D-erythritol 4-phosphate pathway. Plant Cell **17:** 628–643.

Hafrén, A., Hofius, D., Rönnholm, G., Sonnewald, U., and Mäkinen, K. (2010). HSP70 and its cochaperone CPIP promote potyvirus infection in *Nicotiana benthamiana* by regulating viral coat protein functions. Plant Cell **22:** 523–535.

Hans, J., Hause, B., Strack, D., and Walter, M.H. (2004). Cloning, characterization, and immunolocalization of a mycorrhiza-inducible 1-deoxy-d-xylulose 5-phosphate reductoisomerase in arbuscule-containing cells of maize. Plant Physiol. **134:** 614–624.

Hayes, S.A., and Dice, J.F. (1996). Roles of molecular chaperones in protein degradation. J. Cell Biol. **132:** 255–258.

Hemmerlin, A. (2013). Post-translational events and modifications regulating plant enzymes involved in isoprenoid precursor biosynthesis. Plant Sci. **203-204:** 41–54.

Huang, H.C., Sherman, M.Y., Kandror, O., and Goldberg, A.L. (2001). The molecular chaperone DnaJ is required for the degradation of a soluble abnormal protein in *Escherichia coli*. J. Biol. Chem. **276:** 3920–3928.

Kampinga, H.H., and Craig, E.A. (2010). The HSP70 chaperone machinery: J proteins as drivers of functional specificity. Nat. Rev. Mol. Cell Biol. **11:** 579–592.

Karimi, M., Inzé, D., and Depicker, A. (2002). GATEWAY vectors for Agrobacterium-mediated plant transformation. Trends Plant Sci. **7:** 193–195.

Kato, Y., and Sakamoto, W. (2010). New insights into the types and function of proteases in plastids. Int. Rev. Cell Mol. Biol. **280:** 185–218.

Kato, Y., Sun, X., Zhang, L., and Sakamoto, W. (2012). Cooperative D1 degradation in the photosystem II repair mediated by chloroplastic proteases in Arabidopsis. Plant Physiol. **159:** 1428–1439.

Kim, J., Rudella, A., Ramirez Rodriguez, V., Zybailov, B., Olinares, P.D., and van Wijk, K.J. (2009). Subunits of the plastid ClpPR protease complex have differential contributions to embryogenesis, plastid biogenesis, and plant development in *Arabidopsis*. Plant Cell **21:** 1669–1692.

Kuzuyama, T., Takahashi, S., Watanabe, H., and Seto, H. (1998). Direct formation of 2-C-methyl-D-erythritol 4-phosphate from 1-Deoxy-D-xylulose 5-phosphate by 1-Deoxy-D-xylulose 5-phosphate reductoisomerase, a new enzyme in the non-mevalonate pathway to isopentenyl diphosphate. Tetrahedron Lett. **39:** 4509–4512.

Lange, B.M., Wildung, M.R., McCaskill, D., and Croteau, R. (1998). A family of transketolases that directs isoprenoid biosynthesis via a mevalonate-independent pathway. Proc. Natl. Acad. Sci. USA **95:** 2100–2104.

Laule, O., Fürholz, A., Chang, H.S., Zhu, T., Wang, X., Heifetz, P.B., Gruissem, W., and Lange, M. (2003). Crosstalk between cytosolic and plastidial pathways of isoprenoid biosynthesis in *Arabidopsis thaliana*. Proc. Natl. Acad. Sci. USA **100:** 6866–6871.

Lee, S., Lee, D.W., Lee, Y., Mayer, U., Stierhof, Y.D., Lee, S., Jürgens, G., and Hwang, I. (2009). Heat shock protein cognate 70-4 and an E3 ubiquitin ligase, CHIP, mediate plastid-destined precursor degradation through the ubiquitin-26S proteasome system in *Arabidopsis*. Plant Cell **21:** 3984–4001.

Lichtenthaler, H.K., and Wellburn, A.R. (1983). Determination of total carotenoids and chlorophylls a and b of leaf extracts in different solvents. Biochem. Soc. Trans. **603:** 591–592.

Lin, B.L., Wang, J.S., Liu, H.C., Chen, R.W., Meyer, Y., Barakat, A., and Delseny, M. (2001). Genomic analysis of the Hsp70 superfamily in *Arabidopsis thaliana*. Cell Stress Chaperones **6:** 201–208.

Liu, C., Willmund, F., Golecki, J.R., Cacace, S., Hess, B., Markert, C., and Schroda, M. (2007). The chloroplast HSP70B-CDJ2-CGE1 chaperones catalyse assembly and disassembly of VIPP1 oligomers in Chlamydomonas. Plant J. **50:** 265–277.

Lois, L.M., Campos, N., Putra, S.R., Danielsen, K., Rohmer, M., and Boronat, A. (1998). Cloning and characterization of a gene from *Escherichia coli* encoding a transketolase-like enzyme that catalyzes the synthesis of D-1-deoxyxylulose 5-phosphate, a common precursor for isoprenoid, thiamin, and pyridoxol biosynthesis. Proc. Natl. Acad. Sci. USA **95:** 2105–2110.

Lois, L.M., Rodríguez-Concepción, M., Gallego, F., Campos, N., and Boronat, A. (2000). Carotenoid biosynthesis during tomato fruit development: Regulatory role of 1-deoxy-D-xylulose 5-phosphate synthase. Plant J. **22:** 503–513.

Lu, S., et al (2006). The cauliflower Or gene encodes a DnaJ cysteine-rich domain-containing protein that mediates high levels of beta-carotene accumulation. Plant Cell **18:** 3594–3605.

Madueño, F., Napier, J.A., and Gray, J.C. (1993). Newly imported Rieske iron-sulfur protein associates with both Cpn60 and Hsp70 in the chloroplast stroma. Plant Cell **5:** 1865–1876.

Mahmoud, S.S., and Croteau, R.B. (2001). Metabolic engineering of essential oil yield and composition in mint by altering expression of deoxyxylulose phosphate reductoisomerase and menthofuran synthase. Proc. Natl. Acad. Sci. USA **98:** 8915–8920.

Mandel, M.A., Feldmann, K.A., Herrera-Estrella, L., Rocha-Sosa, M., and León, P. (1996). CLA1, a novel gene required for chloroplast development, is highly conserved in evolution. Plant J. **9:** 649–658.

Matsue, Y., Mizuno, H., Tomita, T., Asami, T., Nishiyama, M., and Kuzuyama, T. (2010). The herbicide ketoclomazone inhibits 1-deoxy-D-xylulose 5-phosphate synthase in the 2-C-methyl-D-erythritol 4-phosphate pathway and shows antibacterial activity against *Haemophilus influenzae*. J. Antibiot. **63:** 583–588.

Miernyk, J.A. (2001). The J-domain proteins of *Arabidopsis thaliana*: An unexpectedly large and diverse family of chaperones. Cell Stress Chaperones **6:** 209–218.

Muñoz-Bertomeu, J., Arrillaga, I., Ros, R., and Segura, J. (2006). Up-regulation of 1-deoxy-D-xylulose-5-phosphate synthase enhances production of essential oils in transgenic spike lavender. Plant Physiol. **142:** 890–900.

Ni, M., Tepperman, J.M., and Quail, P.H. (1999). Binding of phytochrome B to its nuclear signalling partner PIF3 is reversibly induced by light. Nature **400:** 781–784.

Nordhues, A., Miller, S.M., Mühlhaus, T., and Schroda, M. (2010). New insights into the roles of molecular chaperones in Chlamydomonas and Volvox. Int. Rev. Cell Mol. Biol. **285:** 75–113.

Ohad, N., Shichrur, K., and Yalovsky, S. (2007). The analysis of protein-protein interactions in plants by bimolecular fluorescence complementation. Plant Physiol. **145:** 1090–1099.

Phillips, M.A., León, P., Boronat, A., and Rodríguez-Concepción, M. (2008). The plastidial MEP pathway: Unified nomenclature and resources. Trends Plant Sci. **13:** 619–623.

Pulido, P., Perello, C., and Rodriguez-Concepcion, M. (2012). New insights into plant isoprenoid metabolism. Mol. Plant **5:** 964–967.

Rajan, V.B., and D'Silva, P. (2009). *Arabidopsis thaliana* J-class heat shock proteins: cellular stress sensors. Funct. Integr. Genomics **9:** 433–446.

Ratnayake, R.M., Inoue, H., Nonami, H., and Akita, M. (2008). Alternative processing of *Arabidopsis* Hsp70 precursors during protein import into chloroplasts. Biosci. Biotechnol. Biochem. **72:** 2926–2935.

Rodriguez, F., Arsène-Ploetze, F., Rist, W., Rüdiger, S., Schneider-Mergener, J., Mayer, M.P., and Bukau, B. (2008). Molecular basis for regulation of the heat shock transcription factor sigma32 by the DnaK and DnaJ chaperones. Mol. Cell **32:** 347–358.

Rodríguez-Concepción, M. (2006). Early steps in isoprenoid biosynthesis: Multilevel regulation of the supply of common precursors in plant cells. Phytochem. Rev. **5:** 1–15.

Rodríguez-Concepción, M., Ahumada, I., Diez-Juez, E., Sauret-Güeto, S., Lois, L.M., Gallego, F., Carretero-Paulet, L., Campos, N., and Boronat, A. (2001). 1-Deoxy-D-xylulose 5-phosphate reductoisomerase and plastid isoprenoid biosynthesis during tomato fruit ripening. Plant J. **27:** 213–222.

Rodríguez-Concepción, M., and Boronat, A. (2002). Elucidation of the methylerythritol phosphate pathway for isoprenoid biosynthesis in bacteria and plastids. A metabolic milestone achieved through genomics. Plant Physiol. **130:** 1079–1089.

Rodríguez-Villalón, A., Gas, E., and Rodríguez-Concepción, M. (2009). Phytoene synthase activity controls the biosynthesis of carotenoids and the supply of their metabolic precursors in dark-grown *Arabidopsis* seedlings. Plant J. **60:** 424–435.

Sakr, S., Cirinesi, A.M., Ullers, R.S., Schwager, F., Georgopoulos, C., and Genevaux, P. (2010). Lon protease quality control of presecretory proteins in *Escherichia coli* and its dependence on the SecB and DnaJ (Hsp40) chaperones. J. Biol. Chem. **285:** 23506–23514.

Sauret-Güeto, S., Botella-Pavía, P., Flores-Pérez, U., Martínez-García, J.F., San Román, C., León, P., Boronat, A., and Rodríguez-Concepción, M. (2006). Plastid cues posttranscriptionally regulate the accumulation of key enzymes of the methylerythritol phosphate pathway in Arabidopsis. Plant Physiol. **141:** 75–84.

Schwender, J., Müller, C., Zeidler, J., and Lichtenthaler, H.K. (1999). Cloning and heterologous expression of a cDNA encoding 1-deoxy-D-xylulose-5-phosphate reductoisomerase of *Arabidopsis thaliana*. FEBS Lett. **455:** 140–144.

Shi, L.X., and Theg, S.M. (2010). A stromal heat shock protein 70 system functions in protein import into chloroplasts in the moss *Physcomitrella patens*. Plant Cell **22:** 205–220.

Sprenger, G.A., Schörken, U., Wiegert, T., Grolle, S., de Graaf, A.A., Taylor, S.V., Begley, T.P., Bringer-Meyer, S., and Sahm, H. (1997). Identification of a thiamin-dependent synthase in *Escherichia coli* required for the formation of the 1-deoxy-D-xylulose 5-phosphate precursor to isoprenoids, thiamin, and pyridoxol. Proc. Natl. Acad. Sci. USA **94:** 12857–12862.

Su, P.H., and Li, H.M. (2008). Arabidopsis stromal 70-kD heat shock proteins are essential for plant development and important for thermotolerance of germinating seeds. Plant Physiol. **146:** 1231–1241.

Su, P.H., and Li, H.M. (2010). Stromal Hsp70 is important for protein translocation into pea and *Arabidopsis* chloroplasts. Plant Cell **22:** 1516–1531.

Sung, D.Y., Kaplan, F., and Guy, C.L. (2001). Plant Hsp70 molecular chaperones: Protein structure, gene family, expression and function. Physiol. Plant. **113:** 443–451.

Takahashi, S., Kuzuyama, T., Watanabe, H., and Seto, H. (1998). A 1-deoxy-D-xylulose 5-phosphate reductoisomerase catalyzing the formation of 2-C-methyl-D-erythritol 4-phosphate in an alternative nonmevalonate pathway for terpenoid biosynthesis. Proc. Natl. Acad. Sci. USA **95:** 9879–9884.

Tanz, S.K., Kilian, J., Johnsson, C., Apel, K., Small, I., Harter, K., Wanke, D., Pogson, B., and Albrecht, V. (2012). The SCO2 protein disulphide isomerase is required for thylakoid biogenesis and interacts with LHCB1 chlorophyll a/b binding proteins which affects chlorophyll biosynthesis in *Arabidopsis* seedlings. Plant J. **69:** 743–754.

Tsai, J., and Douglas, M.G. (1996). A conserved HPD sequence of the J-domain is necessary for YDJ1 stimulation of Hsp70 ATPase activity at a site distinct from substrate binding. J. Biol. Chem. **271:** 9347–9354.

Tsugeki, R., and Nishimura, M. (1993). Interaction of homologues of Hsp70 and Cpn60 with ferredoxin-NADP+ reductase upon its import into chloroplasts. FEBS Lett. **320:** 198–202.

Vitha, S., Froehlich, J.E., Koksharova, O., Pyke, K.A., van Erp, H., and Osteryoung, K.W. (2003). ARC6 is a J-domain plastid division protein and an evolutionary descendant of the cyanobacterial cell division protein Ftn2. Plant Cell **15:** 1918–1933.

Voos, W. (2013). Chaperone-protease networks in mitochondrial protein homeostasis. Biochim. Biophys. Acta **1833:** 388–399.

Wall, D., Zylicz, M., and Georgopoulos, C. (1994). The NH2-terminal 108 amino acids of the *Escherichia coli* DnaJ protein stimulate the ATPase activity of DnaK and are sufficient for lambda replication. J. Biol. Chem. **269:** 5446–5451.

Wickner, S., Maurizi, M.R., and Gottesman, S. (1999). Posttranslational quality control: Folding, refolding, and degrading proteins. Science **286:** 1888–1893.

Yalovsky, S., Paulsen, H., Michaeli, D., Chitnis, P.R., and Nechushtai, R. (1992). Involvement of a chloroplast HSP70 heat shock protein in the integration of a protein (light-harvesting complex protein precursor) into the thylakoid membrane. Proc. Natl. Acad. Sci. USA **89:** 5616–5619.

Zeidler, J., Schwender, J., Mueller, C., and Lichtenthaler, H.K. (2000). The non-mevalonate isoprenoid biosynthesis of plants as a test system for drugs against malaria and pathogenic bacteria. Biochem. Soc. Trans. **28:** 796–798.

Zybailov, B., Friso, G., Kim, J., Rudella, A., Rodríguez, V.R., Asakura, Y., Sun, Q., and van Wijk, K.J. (2009). Large scale comparative proteomics of a chloroplast Clp protease mutant reveals folding stress, altered protein homeostasis, and feedback regulation of metabolism. Mol. Cell. Proteomics **8:** 1789–1810.